Progress In Electromagnetics Research, PIER 37, 221–234, 2002

STUDY ON THE TWO-FREQUENCY SCATTERING CROSS SECTION AND PULSE BROADENING OF THE ONE-DIMENSIONAL FRACTAL SEA SURFACE AT MILLIMETER WAVE FREQUENCY

L. Guo

School of Science
Xidian University
Xi'an 710071, Shaanxi Province, P. R. China

C. Kim

Department of Electronics
Kyungpook National University
Taegu 702-701, Korea

Abstract—Based on the Kirchhoff approximation for the surfaces with small slopes, the pulse beam wave scattering from the one-dimensional fractal sea surface with the actual spectrum is studied. The influence of the different fractal dimension, incident angle, and the center frequency on the distributions of the two-frequency scattering cross section is analyzed. The numerical result shows that there exists the largest coherence bandwidth for the two-frequency scattering cross section at the specular direction. The coherence bandwidth will increase with the decrease of the fractal dimension and with the increase of the incident angle and the center frequency, as well. It is also found that the scattering power takes a pulse shape, but with a pulse broadening for the incident power being δ function, this pulse broadening is inversely proportional to the coherence bandwidth.

1. INTRODUCTION

The study of the electromagnetic scattering from rough surfaces with a plane wave and beam incidence has received considerable attention for the past several decades. Among the analytical research, pulse beam scattering is the most useful research for many applications, such as electromagnetic measuring of the surface roughness, laser beam scattering from the complex environment and the ocean acoustic scattering in sonar systems. The presence of the surface roughness affects the scattering wave by introducing the time delay and the shape of the pulse beam. Some of the previous works of the time-dependent scattering from the rough surface have been limited to studying the reflected wave observed in the specular direction [1]. Up to now, there has also been a strong interest in many optical and millimeter wave experiments for roughness sensing, utilizing the angular and frequency correlations of the scattering wave [2–4]. Recently, in order to obtain the information of the earth's surface by using SAR with interferometric technique incorporated, many researchers have devoted themselves to the study of the coherence bandwidth and pulse broadening of the electromagnetic waves scattering from the rough surface with the pulse beam incidence [5, 6]. A. Ishimaru et al., presented analytical expressions for the two-frequency mutual coherence function and angular correlation function of the scattered wave from one-dimensional rough surfaces by the first and second Kirchhoff approximation [7, 8]. The pulse broadening and backscattering enhancement are also discussed.

In this paper, based on the theoretical result of the pulse beam scattering from the rough surface proposed by A. Ishimaru, we focus our investigation on the pulse beam wave scattering from the one-dimensional fractal sea surface at millimeter wave frequency with the actual spectrum of the sea considered. The distributions of the two-frequency scattering cross section and the scattering power with different fractal dimension, incident angle, and center frequency are analyzed. The dependence of the coherence bandwidth and the pulse broadening on the fractal dimension and incident angle are discussed in detail.

2. FORMULATION OF THE TWO-FREQUENCY SCATTERING CROSS SECTION AND SCATTERING POWER FROM THE ROUGH SURFACE

Consider an incident pulse beam $E_i(t)$ impinging on a one-dimensional rough surface characterized by the function $z = \zeta(x)$, extending from

$x = -L/2$ to $x = L/2$. We assume the incident center frequency is f and the incident angle θ_i. Based on the first-order Kirchhoff approximation for the surfaces with small slopes [7, 9] (in this case the rms slopes $s = \sqrt{2}\delta/l < 0.5$ and the correlation length $l \geq \lambda$, where δ is the rms height of the surface), the scattering field in the far region can be expressed as:

$$E_s = k\cos\theta_s\sqrt{\frac{2\pi}{kR}}\exp(ikR - i\pi/4)T(\mathbf{K}_s, \mathbf{K}_i) \tag{1}$$

where $k = 2\pi/\lambda$ is the incident wave number, θ_s is the scattering angle, R is the distance from the origin to the observation point and the transition matrix T is given by [7, 8]:

$$T(\mathbf{K}_i, \mathbf{K}_s) = \frac{F_1}{2\pi}\int R_1 \exp\left[-i(\mathbf{K}_s - \mathbf{K}_i)\cdot\mathbf{r}_1\right] dx_1 \tag{2}$$

Here R_1 is the local Fresnel reflection coefficient at $\mathbf{r}_1 = x_1\hat{x} + \zeta_1\hat{z}$. The incident vector $\mathbf{K}_i$ and the scattering vector $\mathbf{K}_s$, and F_1 can be written as:

$$\mathbf{K}_{i,s} = k\sin\theta_{i,s}\hat{x} \pm k\cos\theta_{i,s}\hat{z}, \quad F_1 = \frac{1 - \sin\theta_i\sin\theta_s + \cos\theta_i\cos\theta_s}{(\cos\theta_i + \cos\theta_s)\cos\theta_s} \tag{3}$$

where "±" indicates the incident case (subscript i) and the scattering case (subscript s), respectively. The two-frequency scattering cross section per unit area of the rough surface is defined as [7]:

$$\sigma^0(\mathbf{K}_i, \mathbf{K}_s; \mathbf{K}'_i, \mathbf{K}'_s) = \sigma^0(\omega, \omega') = (R/L) < E_s E'^*_s > \tag{4}$$

where

$$\mathbf{K}'_{i,s} = k'\sin\theta'_{i,s}\hat{x} \pm k'\cos\theta'_{i,s}\hat{z} \tag{5}$$

In the above expression, $k = 2\pi f/c = \omega/c$ and $k' = 2\pi f'/c = \omega'/c$. Substituting Eq. (1) and Eq. (2) into Eq. (4), we obtain

$$\sigma^0 = 2\pi\sqrt{kk'}\cos\theta_s\cos\theta'_s(< T(\omega)T'^*(\omega') > /L)\exp[i(k - k')R] \tag{6}$$

where $<T(\omega)T'^*(\omega')>$ is the two-frequency mutual coherence function. It is usually denoted by $\Gamma(\omega, \omega')$. In the Kirchhoff approximation for the rough surface with small slopes, R_1 can be approximated by the Fresnel reflection coefficient for a flat surface, it is a constant for a fixed incident angle and can be taken outside the integral in Eq. (2), thus Eq. (2) can be rewritten as:

$$T = H_1 \int \exp(-i\mathbf{v}\cdot\mathbf{r}_1) dx_1 \tag{7}$$

where $H_1 = F_1 R_1/(2\pi)$, $\mathbf{v} = \mathbf{K}_s - \mathbf{K}_i = v_x\hat{x} + v_z\hat{z}$, $v_x = k(\sin\theta_s - \sin\theta_i)$, $v_z = k(\cos\theta_s + \cos\theta_i)$. Based on the Kirchhoff approximation of the rough surfaces with small slopes, the two-frequency mutual coherence function is found to be [7, 8]

$$\begin{aligned}\Gamma(\omega,\omega') &= < T(\omega)T'^*(\omega') > \\ &= H_1 H_1' \int dx_1 \int [< \exp(-i\mathbf{v}\cdot\mathbf{r}_1 + i\mathbf{v}'\cdot\mathbf{r}_1') > \\ &\quad - < \exp(-i\mathbf{v}\cdot\mathbf{r}_1) >< \exp(-i\mathbf{v}'\cdot\mathbf{r}_1')]\, dx_1' \end{aligned} \tag{8}$$

If the height of $\zeta(x)$ is assumed to satisfy the Gaussian distribution, we have [1, 7]

$$< \exp(-iv_z\zeta_1 + iv_z'\zeta_1') >= \exp\left\{-\left[\left(v_z^2 + v_z'^2\right)\delta^2/2 - v_z v_z' < \zeta_1\zeta_1' >\right]\right\} \tag{9}$$

where $< \zeta_1\zeta_1' >=< \zeta(x_1)\zeta(x_1') >= G(x_1 - x_1') = G(x_d)$ is the auto-correlation function of $\zeta(x)$. Making use of the coordinates transformation for the integral variable x_1 and x_1' by $x_d = x_1 - x_1'$, $x_c = (x_1 + x_1')/2$, we get the following identities [7, 8]:

$$\int dx_1 \int dx_1' = \int dx_d \int dx_c \tag{10a}$$

$$\exp(-iv_x x_1 + iv_x' x_1') = \exp\left[-i(v_d x_c + v_c x_d)\right] \tag{10b}$$

where $v_d = v_x - v_x' = k(\sin\theta_s - \sin\theta_i) - k'(\sin\theta_s' - \sin\theta_i')$, $v_c = (v_x + v_x')/2$. Substituting Eq. (8)–Eq. (10) into Eq. (6), the two-frequency scattering cross section can be simplified as follows:

$$\sigma^0 = 2\pi\sqrt{kk'}\cos\theta_s\cos\theta_s' H_1 H_1' \phi_1\phi_2 \exp\left[i(k - k')R\right] \tag{11}$$

where

$$\phi_1 = \frac{1}{L}\int_{-\infty}^{\infty} \exp\left(-\pi x_c^2/L^2\right)\exp(-iv_d x_c)dx_c = \exp\left(-v_d^2 L^2/4\pi\right) \tag{12}$$

$$\phi_2 = \exp\left[-(v_z^2 + v_z'^2)\delta^2/2\right]\sum_{n=1}^{\infty}\frac{(v_z v_z'\delta^2)^n}{n!}\int_{-\infty}^{\infty}[G(x_d)]^n \exp(-iv_x x_d)dx_d \tag{13}$$

When $k = k'$, $\theta_i = \theta_i'$, $\theta_s = \theta_s'$ in Eq. (11), this equation will reduce to the conventional Kirchhoff approximation expression of the bistatic scattering cross section for the case of the continued wave incidence. Once the two-frequency mutual coherence function $\Gamma(\omega,\omega')$ of Eq. (8) is obtained, the scattering power $P_s(t)$, often encountered and used in the measurement, can also be obtained. As far as the incident pulse

beam is concerned, the incident power can be expressed as the Fourier transform:

$$P_i(t) = < E_i(t)E_i^*(t) > = \frac{1}{(2\pi)^2}\iint \overline{E}_i(\omega)\overline{E}_i^*(\omega')\exp(-i\omega t + i\omega' t)d\omega d\omega'$$
$$= \frac{1}{2\pi}\int P_i(\omega_d)\exp(-i\omega_d t)d\omega_d \tag{14}$$

where

$$P_i(\omega_d) = \int P_i(t)\exp(i\omega_d t)dt = \frac{1}{2\pi}\int \overline{E}_i(\omega)\overline{E}_i^*(\omega')d\omega_c \tag{15}$$

Here we also used the variable replaced by $\omega_d = \omega - \omega'$, $\omega_c = (\omega + \omega')/2$. Therefore, the scattering power can be written as the following:

$$P_s(t) = < E_s(t)E_s^*(t) > = \frac{1}{(2\pi)^2}\iint \Gamma(\omega,\omega')\overline{E}_i(\omega)\overline{E}_i^*(\omega')\exp(-i\omega_d t)d\omega_d d\omega_c$$
$$= \frac{1}{2\pi}\int \Gamma(\omega_d)P_i(\omega_d)\exp(-i\omega_d t)d\omega_d \tag{16}$$

In the above derivations, the transformation of equation $\overline{E}_s(\omega) = T(\omega)\overline{E}_i(\omega)$ has been utilized [7, 8]. From Eq. (15) and Eq. (16), it is found that after obtaining the calculating result of $\Gamma(\omega,\omega')$, the scattering power can be acquired with the incident power already known. If $P_i(t)$ is assumed to be the δ function, i.e., $P_i(t) = \delta(t)$, then from Eq. (15) we have $P_i(\omega_d) = 1$. Hence according to Eq. (16), the scattering power $P_s(t)$ is just the Fourier transform of the two-frequency mutual coherence function.

3. NUMERICAL RESULT FOR THE FRACTAL SEA SURFACE

In this section we numerically calculate the electromagnetic scattering from the fractal sea surface with the pulse beam wave incidence. The analytical expression of the fractal model for the rough sea surface is represented as follows [10, 11]:

$$\zeta(x) = \frac{\sqrt{2}\delta\left[D(2-D)\right]^{1/2}}{\left[1-(D-1)^{2N}\right]^{1/2}}\sum_{m=1}^{M} W_{PM}(\kappa_m)\sum_{n=N_1}^{N_2}(D-1)^n\sin\left(KY^n\kappa_m x + \phi_n\right) \tag{17}$$

where δ is the standard rms height of the fractal surface and $D(1 < D < 2)$ represents the box-counting fractal dimension of the surface,

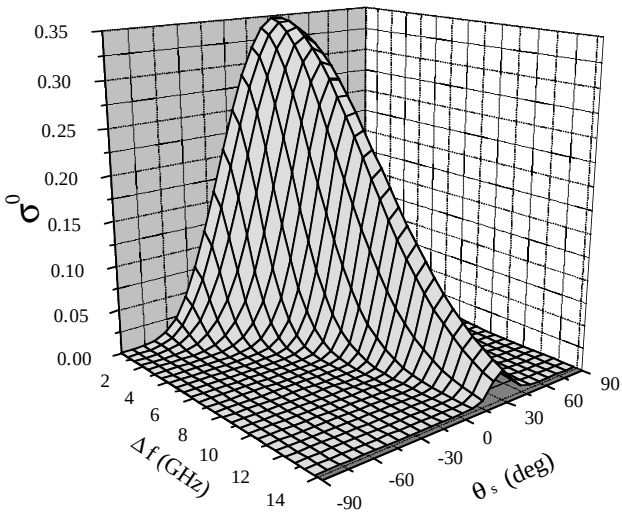

Figure 1. The distribution of σ^0 with $D = 1.5,\ \theta_i = 30^\circ,\ f = 75\,\mathrm{GHz}$.

a larger D results in a rougher surface. K is the fundamental wavenumber and b is the fundamental spatial frequency. $N(N = N_2 - N_1 + 1)$ and M are the numbers of tones and ϕ_n is a phase term that has a uniform distribution over the interval $[-\pi, \pi]$. $P_{PM}(f)$ is the Pierson-Moskowitz (PM) spectrum of the sea surface, given by [12]:

$$W_{PM}(\kappa) = \frac{\alpha_p g^2}{(2\pi)^4 \kappa^5} \exp\left[-1.25\left(\frac{\kappa_{PM}}{\kappa}\right)^4\right] \tag{18}$$

where the Philips constant $\alpha_p = 0.0081$, the frequency $\kappa_{PM} = 0.13g/u_w$, u_w is the mean wind speed over the water, $g = 9.8\,\mathrm{m/s^2}$, and $\{\kappa_m\}_{m=1}^{M}$ are the frequency points at which the Pierson-Moskowitz spectrum is uniformly sampled. This fractal sea model has already been proved to satisfy the Gaussian distribution.

We first calculate the two-frequency scattering cross section σ^0 of the fractal sea surface by Eq. (11) with the pulse beam incidence at millimeter wave frequency. In performing the calculation, $\theta_i = \theta_i'$, $\theta_s = \theta_s'$, the incident center frequency is set to be 75 GHz, the parameters in the rough fractal model of Eq. (17) are given by $b = \sqrt{e}$, $K = 1/(2\lambda)$, $u_w = 8\,\mathrm{m/s}$, $\delta = 0.5\lambda$, $N_1 = 0$, $N_2 = 9$, $M = 30$, the dielectric constant $\varepsilon_r = (48.3, 34.9)$ [9] and the illuminating distance $L = 40\lambda$.

In Fig. 1, the distribution of the two-frequency scattering cross section vs different frequency difference $\Delta f = f' - f$ and scattering

angle θ_s is depicted for HH polarization (VV case can be evaluated in a similar way) with incident angle $\theta_i = 30^\circ$ and fractal dimension $D = 1.5$. It should be pointed out that for the case of $D = 1.5$, the correlation length can be computed and the result is $l = 2.3\lambda$ [13], thus the corresponding rms slope $s = 0.31$. Hence the conventional scalar first-order Kirchhoff approximation with small slopes of the surface is valid for this case. It is readily found that the two-frequency scattering cross section σ^0 has the maximum value when $f = f'(\Delta f = 0)$ for the same scattering angle. With increasing the frequency difference Δf, σ^0 will decrease from the peak value to zero at a different rate for the different scattering angle. It is observed that σ^0 decreases at a more gentle rate in the specular direction, and the amplitude of σ° and the coherence bandwidth (the corresponding Δf for σ^0 decreases from the maximum value to zero [7]) also have the largest values. When the scattering direction is off the specular direction, σ^0 will decrease rapidly with increasing Δf, and the coherence bandwidth will also decrease. Fig. 2 shows the distribution of σ^0 for different Δf and different θ_s, but with fractal dimension $D = 1.3$ (the corresponding $l = 2.6\lambda$, $s = 0.27$), the other parameters are the same as those in Fig. 1. It is shown that the coherence bandwidth increases at the specular direction for the small value of D compared with that in Fig. 1.

Fig. 3 also illustrates the distribution of σ^0 with $D = 1.5$ but with the incident angle $\theta_i = 60^\circ$. Analogous to the analysis of Fig. 1, there also exists the largest coherence bandwidth at the specular direction. Fig. 4 presents the distribution of σ^0 with the center frequency $f = 50\,\mathrm{GHz}$, and $D = 1.5$, $\theta_i = 30^\circ$. It is obvious that both of the amplitude of σ^0 and the coherence bandwidth will decrease with the decrease of center frequency compared with those in Fig. 1.

In order to further check the formulation of the two-frequency scattering cross section given in section 2, we consider the calculated behavior of the scattering angular distribution of σ^0 with $\Delta f = 0$ ($f = f'$) for different D and θ_i in Fig. 5. In this case, the result of σ^0 will reduce to that of the conventional Kirchhoff approximation with the continued wave incidence. In this figure, the comparison of the present calculations with the Monte Carlo simulation for σ^0 is also given with $\theta_i = 30^\circ$, $D = 1.5$. In performing the calculation of the Monte Carlo technique [14], the number of the sampling surfaces is set to be 100, and the sampling number of each surface is 2048. It is obvious that the two methods are in fairly good agreement. From Fig. 5, we can also observe that the distribution of σ^0 will be different for different D and θ_i, and for the same fractal dimension and scattering angle, the larger the incident angle, the smaller the value of σ^0 will be. Fig. 6 shows the comparison of the distribution of σ^0 with varying of the

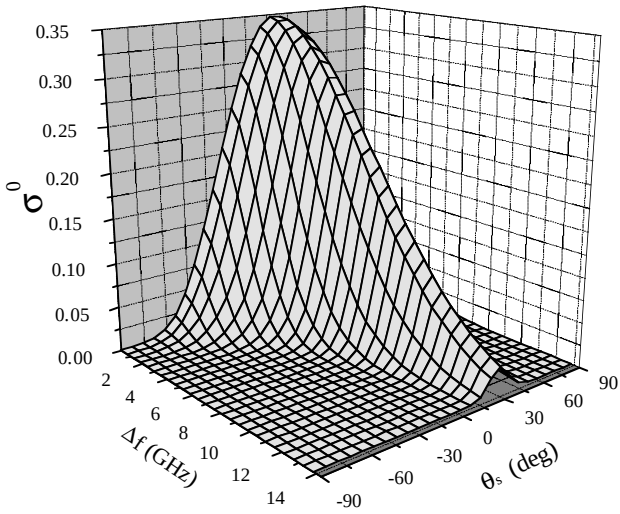

Figure 2. The distribution of σ^0 with $D = 1.3,\ \theta_i = 30°,\ f = 75\,\mathrm{GHz}$.

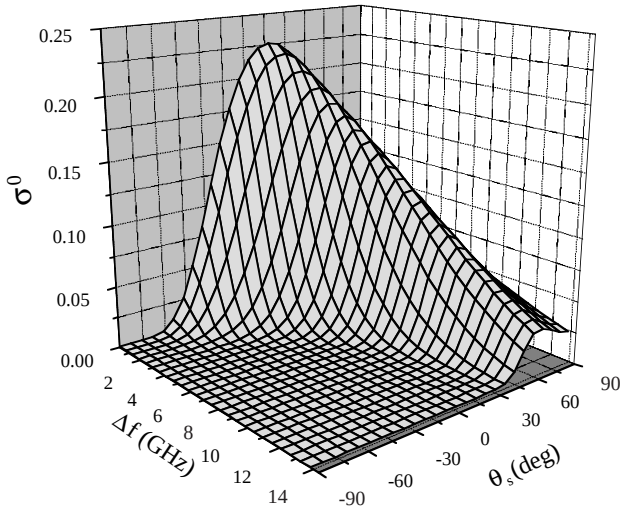

Figure 3. The distribution of σ^0 with $D = 1.5,\ \theta_i = 60°,\ f = 75\,\mathrm{GHz}$.

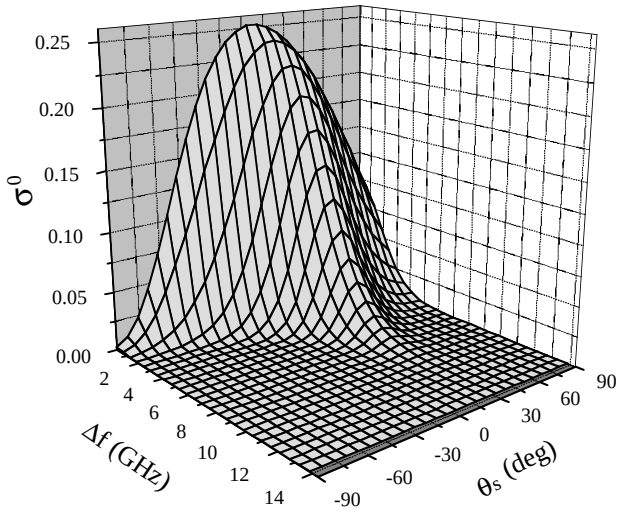

Figure 4. The distribution of σ^0 with $D = 1.5,\ \theta_i = 30°,\ f = 50\,\text{GHz}$.

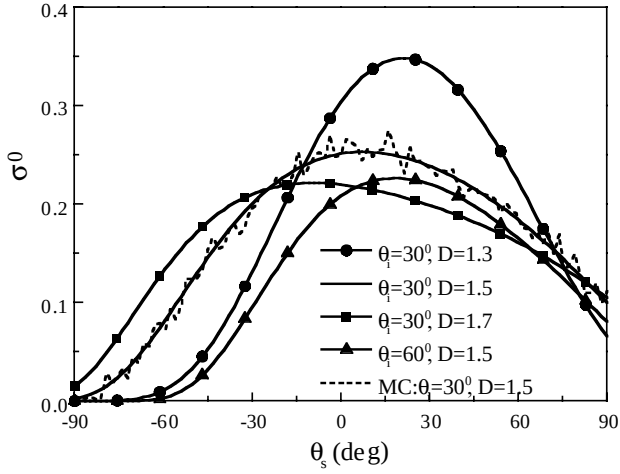

Figure 5. The angular distribution of σ^0 for different D and θ_i with $f = f'$.

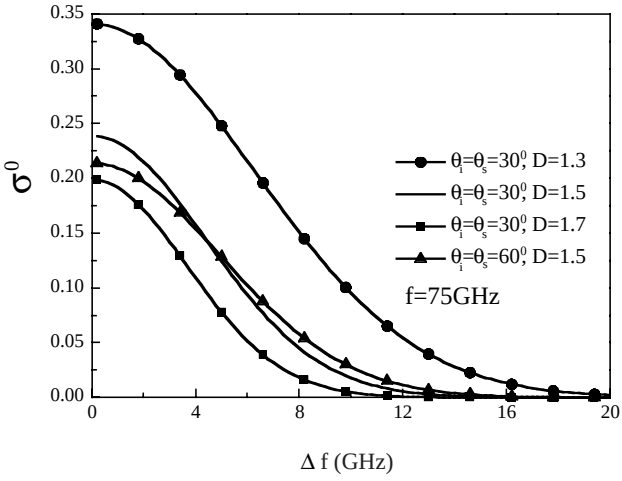

Figure 6. σ^0 versus the frequency difference Δf for different D and θ_i at the specular direction.

frequency difference Δf at specular direction for different D and θ_i, the center frequency $f = 75\,\text{GHz}$. Compared with the results shown in Fig. 1–Fig. 3, it can be seen that the amplitude of σ^0 and the coherence bandwidth decrease with increasing D for the same θ_i and Δf, but with increasing the incident angle, the coherence bandwidth will increase for the same fractal dimension.

Another point worth noting is the characteristic of the scattering power with the pulse beam incidence and our effort is focused on the scattering pulse shape with the time delay. As was mentioned in the theoretical analysis presented in section 2, if we assume $P_i(t) = \delta(t)$, from Eq. (16), it is already known the scattering power $P_s(t)$ will be the Fourier transform of the two-frequency mutual coherence function. Fig. 7 presents the dependence of the scattering power distribution on the time delay and scattering angle with $D = 1.5$, $\theta_i = 30°$, $f = 75\,\text{GHz}$. It is readily observed that the shape of the scattering power is not a δ function, but a pulse with a finite width in the near vertical direction. This phenomenon is just the pulse broadening for the scattering power described by A. Ishimaru. It also shows consistency with the previous experiment results [2, 3]. We can also find that the maximum of the scattering power does not appear in the specular direction, and for the fixed scattering angle, $P_s(t)$ decreases from its maximum value (at $t = 0$) to zero at a different rate.

Fig. 8 shows the scattering power as a function of time delay with different incident angle and fractal dimension at the specular direction.

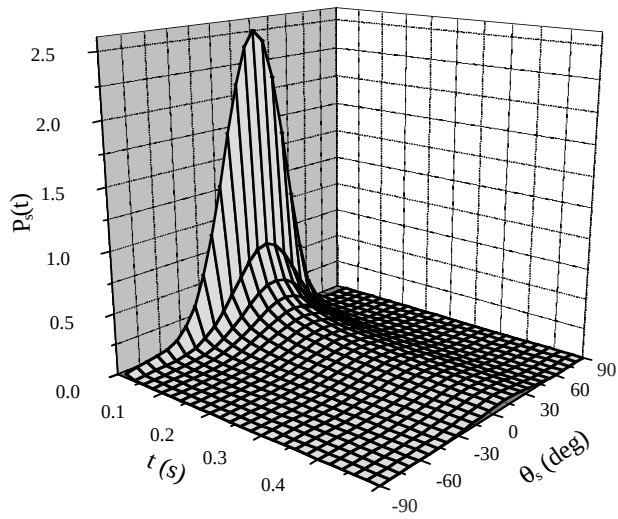

Figure 7. The distribution of the scattering power with $D = 1.5$, $\theta_i = 30^\circ$, $f = 75\,\mathrm{GHz}$.

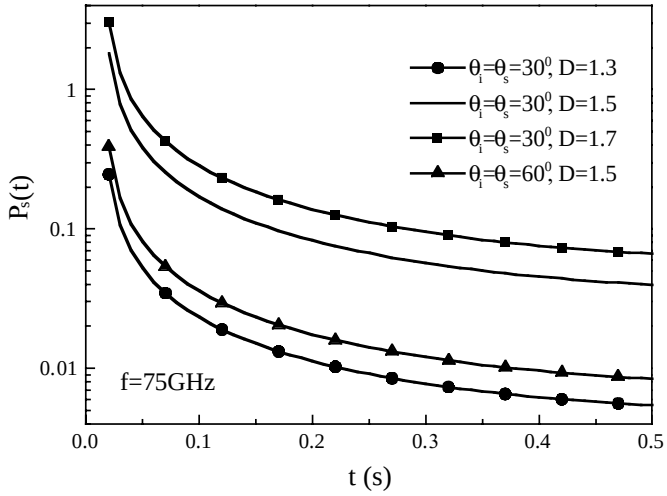

Figure 8. The scattering power as function of time delay with different θ_i and D at the specular direction.

Compared with the curves given in Fig. 6, it is found that for the same incident angle, with increasing the fractal dimension, the amplitude of $P_s(t)$ and the pulse broadening increase, whereas the amplitude of σ° and the coherence bandwidth decrease (shown in Fig. 6). For the same fractal dimension and the small the incident angle (corresponding to the small coherence bandwidth), there also exist a large value for both $P_s(t)$ and the pulse broadening at the specular direction. Hence we conclude that the small coherence bandwidth will correspond to the large pulse broadening. In other words, this pulse broadening is inversely proportional to the coherence bandwidth, this result is also valid for the scattering power at the non-specular direction.

4. CONCLUSIONS AND DISCUSSIONS

In summary, this paper presents the pulse beam wave scattering from the one-dimensional fractal sea surface at the millimeter wave frequency with the actual spectrum considered. According to the Kirchhoff approximation for the surfaces with small slopes given by A. Ishimaru, the analytical solution for the two-frequency cross section is derived for the fractal sea surface with Gaussian distribution. Under the condition of $\Delta f = 0$, the two-frequency cross section can be reduced to the result of the conventional Kirchhoff approximation with the continued wave incidence. Calculations were carried out to examine the influence of the different fractal dimension, incident angle, and center frequency on the distributions of the two-frequency scattering cross section. The numerical result shows that there exists the largest coherence bandwidth for the two-frequency scattering cross section at the specular direction. The coherence bandwidth will increase with the decrease of the fractal dimension and with the increase of the incident angle and the center frequency. It is also found that the scattering power takes a pulse shape, but with a pulse broadening for the incident power being δ function, this pulse broadening is inversely proportional to the coherence bandwidth. It should be noted that the conclusions obtained are valid for both HH and VV polarizations, but our solution is limited to the approximation for surfaces with small rms slope (i.e., surfaces with small and moderate fractal dimension). As the fractal dimension exceeds 1.8 (in this case, $l = 1.4\lambda$, $s = 0.51$), the rms slope will also exceed 0.5, the correlation length will be gradually less than the incident wavelength, and the second-order Kirchhoff approximation should be included to deal with the scattering problem. Further investigation about the two-frequency cross section and the pulse broadening of the scattering power will be necessary for the case of the actual two-dimensional fractal sea surface.

REFERENCES

1. Ogilvy, J. A., *Theory of Wave Scattering from Random Rough Surfaces*, 85, Adam Hilger, Bristol, 1991.
2. O'donnel, K. A. and E. R. Meendez, "Experimental study of scattering from characterized random surfaces," *J. Opt. Soc. Am,* Vol. A4, No. 7, 1194–1205, 1987.
3. Ishimaru, A., "Experimental and theoretical studies on enhanced backscattering from scatterers and rough surfaces," *Scattering in Volumes and Surfaces,* Amsterdam, Elsevier, 1990.
4. Nitta, H. and T. Asakura, "Method for measuring mean particle size of the bulk power using speckle patterns," *Applied Optics*, Vol. 30, No. 33, 4854–4858, 1991.
5. Madsen, S. N., H. A. Zebker, and J. Martin, "Topographic mapping using radar interferometry: processing techniques," *IEEE Trans. Geosci. and Remote Sensing,* Vol. 31, No. 1, 246–256, 1993.
6. Rodriguez, E. and J. Martin, "Theory and design of interferometric synthetic aperture radars," *IEE Proceedings F,* Vol. 139, No. 2, 147–159, 1992.
7. Ishimaru, A., *Wave Propagation and Scattering in Random Media,* Chap. 17, Academic Press, New York, 1978.
8. Ishimaru, A., L. Ailes-Sengers, P. Phu, and D. Winebrenner, "Pulse broadening and two-frequency mutual coherence function of the scattered wave from rough surfaces," *Waves in Random Media,* Vol. 4, No. 2, 139–148, 1994.
9. Ulaby, F. T., R. K. Moore, and A. K. Fung, *Microwave Remote Sensing,* Vol. 2, Chap. 12, Addision-Wesbey Publishing, 1982.
10. Berizzi, F. and E. Dalle-Mese, "Fractal analysis of the signal scattered from the sea surface," *IEEE Trans. on Antennas Propagat.,* Vol. 47, No. 2, 324–338, 1999.
11. Guo, L. and Z. Wu, "Fractal model and electromagnetic scattering from the time-varying sea surface," *IEE of Electronic Letters,* Vol. 36, No. 21, 1810–1812, 2000.
12. Thorsos, E. I., "Acoustic scattering from a 'Pierson-Moskowitz' sea surface," *J. Acoust. Soc. Am.,* Vol. 88, No. 1, 335–349, 1990.
13. Guo, L. and Z. Wu, "Electromagnetic scattering from the time-varying sea surface with considering the distribution of sea power spectrum," *ACTA Electronica Sinica (in Chinese),* Vol. 29, No. 9, 1287–1289, 2001.
14. Thorsos, E. I., "The validity of the Kirchhoff approximation for

rough surface scattering using a Gaussian roughness spectrum," *J. Acoust. Soc. Am.,* Vol. 86, No. 1, 78–92, 1989.